

A RIGOROUS, ENGINEER-FRIENDLY APPROACH FOR MODELING REALISTIC, COMPOSITE ROTOR BLADES

D. H. Hodges* and W. Yu**

* Prof., School of Aerospace Engineering, Georgia Institute of
Technology, Atlanta, Georgia 30332-0150, USA

** Asst. Prof., Dept. of Mechanical & Aerospace Engineering,
Utah State University, Logan, Utah 84322-4130, USA

ABSTRACT

A rigorous approach is presented for the modeling of composite beam structures of the type encountered in wind turbine blades, helicopter rotor blades, and the like. The analysis methodology is based on a dimensional reduction of the geometrically nonlinear, three-dimensional, anisotropic theory of elasticity. Small parameters stemming from the beam-like geometry of slender structures such as wind turbine blades lead to a splitting of the problem into a (usually) linear, two-dimensional cross-sectional analysis and a geometrically-exact nonlinear, one-dimensional beam analysis. The incorporation of such beam analyses into flexible-multi-body codes presents a unified and powerful approach to the modeling of wind turbines with composite rotor blades. The generality and power of the methodology is illustrated in several examples.

1. INTRODUCTION

As most anyone who has tried to analyze composite beams will have found, the numerous published works on the theory of beams for isotropic materials are simply not suitable for application to composite beams. Moreover, straightforward modification of those theories to make them generally applicable is problematic. In an extensive review of the literature on beam theories from the 1940s through the mid-1980s in the book by Hodges (2006), it is found that even the most mathematically sophisticated theories exhibit difficulties when one attempts to apply them to practical problems. The first difficulty is in the formulation of appropriate cross-sectional constitutive laws in terms of known three-dimensional (3D) material constants. Even the most sophisticated of the older theories cannot deal with

phenomena such as elastic couplings from anisotropic materials, initial twist and curvature, or inhomogeneous, built-up construction. The required warping functions associated with all the types of deformation are coupled and complicated. Second, the advanced theories rely heavily on rather abstract tensor analysis, which can be troublesome for applications-oriented engineers.

Since the mid-1980s, techniques have been under development that address both of these issues. Work by Giavotto *et al.* (1983) pioneered cross-sectional analysis of general composite beams using a framework based on linear elasticity. Although Borri and Mantegazza (1985) and Kosmatka and Friedmann (1989) applied such an approach to the nonlinear problem of rotor blade dynamics, a unified approach to rigorously treat geometrically nonlinear problems and restrained warping effects did not turn out to be quickly forthcoming. However, within the last decade there has been significant progress. As a result, the beam theory presented by Hodges (2006) is not only a unified approach, but it is also quite suitable for practical helicopter and wind-turbine rotor blade applications. While it involves a minimal amount of tensor analysis, this only affects the derivation – not the application. It is based on asymptotic procedures that exploit the smallness of parameters such as strain and slenderness, and the resulting one-dimensional (1D) equations are geometrically exact, mnemonic, and can be written in a few lines. Here “geometrically exact” refers to the fact that the finite rotation of the cross-sectional frame is treated exactly, without small-angle approximations. The theory does not make use of an assumed displacement field. Rather, the equations governing the warping fall out from the use of asymptotic methods and can be solved either in closed form or by the finite element method. The constitutive law for the 1D theory along with recovery relations for 3D strain and stress are also derived as part of this procedure. There are neither restrictions on the type of material nor on the geometry of the cross-section.

The lowest-order theory is of the form of the Euler-Kirchhoff-Clebsch theory as far as the measures of deformation are concerned, but it is generalized to include the structural couplings that normally follow from the use of anisotropic materials. The refined theories are of the type that accommodate either transverse shearing deformation for closed cross-sections or the Vlasov effect for open sections.

The keys to extending the older works, so as to create a workable, practical and yet rigorous analysis, were two-fold. First, a kinematical description was developed by Danielson and Hodges (1987) that allows the 3D strain field to be expressed in terms of the intrinsic 1D measures for initially twisted and curved beams. The resulting expressions for 3D strain involve no tensor analysis at all, which facilitates the incorporation of nonlinear effects with no significant increase in complexity. Second, the variational-asymptotic method (VAM) of Berdichevsky (1980) was found to split a 3D geometrically nonlinear elasticity analysis for beam-like structures into a nonlinear 1D analysis and a (usually) linear two-dimensional (2D) analysis. This method also turned out to be amenable to determining the cross-sectional stiffness constants. They could be found in closed form for certain simple cases, generally possible only for either isotropic beams with relatively simple cross-sectional geometries or thin-walled beams made of laminated composite materials. Or they could be found by application of the finite element method in even the most general case. This part of the analysis is referred to as “cross-sectional analysis.”

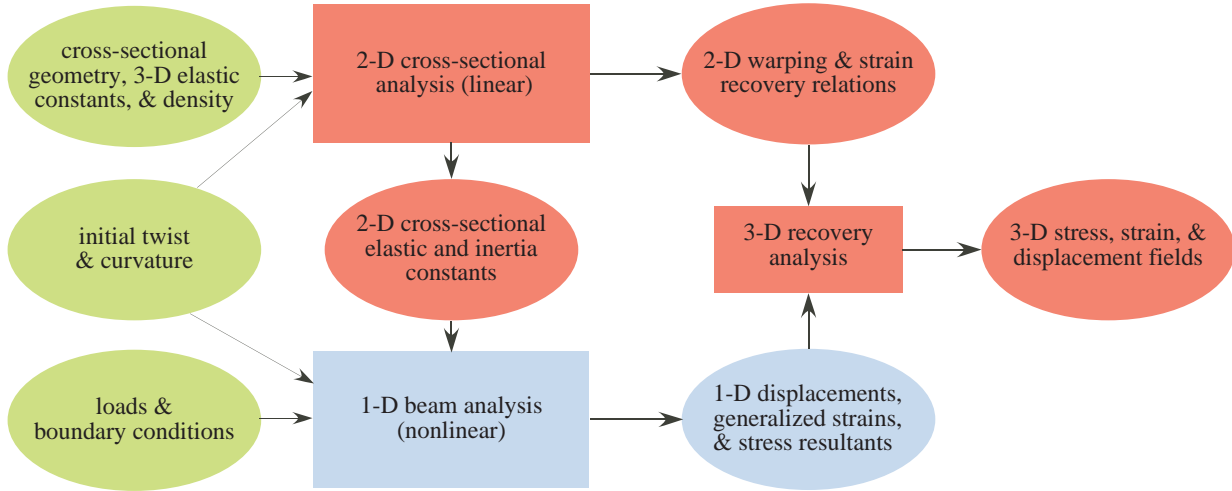


Fig. 1: Beam analysis procedure

In the 1990s, using the 3D strain developed by Danielson and Hodges (1987) and the VAM of Berdichevsky (1980), Hodges and co-workers undertook the creation of a general finite element-based methodology for composite blade cross-sectional analysis as part of the framework for nonlinear beam theory. The result was the finite element code called VABS (the Variational Asymptotic Beam Section analysis). The history of the development and validation of VABS is extensive and can be found in works such as Hodges *et al.* (1992); Cesnik and Hodges (1993, 1994, 1995, 1997); Popescu and Hodges (1999a,b); Volovoi *et al.* (2001); Popescu *et al.* (2000); Cesnik and Shin (2001); Yu *et al.* (2002a,b). See work cited by Hodges (2006) for a more complete history of the development and validation of VABS as well as the corresponding 1D theory of beams. It should be noted that the current version of VABS as of this writing is based on Yu *et al.* (2002a).

Fig. 1 shows the overall beam-modeling process. The ellipses represent bodies of data, and the rectangles represent analyses. Input data sets for the entire process are in green ellipses. The 1D theory and its output are in blue. Finally, the 2D cross-sectional analysis (as a set of formulae or a finite-element-based program such as VABS) and its output are shown in red. The inertia properties are included in the cross-sectional analysis as well, since they are usually written in terms of integrals over the cross-sectional plane. The cross-sectional analysis requires details of the cross-sectional geometry, material elastic constants, and material densities. Initial curvature and twist must be input to both 1D and 2D analyses, while loads and boundary conditions only affect the 1D analysis*. Once the user creates a mesh of the cross-sectional plane and identifies the material properties of each element, then VABS can be run. Its output includes the cross-sectional properties and stress/strain recovery relations (which require output from a 1D analysis). It has been shown that this splitting of the 3D problem leads to two to three orders of magnitude reduction in computational effort relative to that of 3D finite elements, with comparable accuracy of the recovered stresses in the beam interior.

*For rotor blade applications, external pressure from aerodynamics creates surface tractions that are much smaller than stress induced by bending. For surface tractions that are not negligible, the cross-sectional analysis must be adjusted to take them into account.

In this paper we will first address the formulation of the 3D problem. Then, both the 2D cross-sectional and 1D beam analyses are outlined. Finally, results obtained for example problems will be presented and discussed, followed by concluding remarks.

2. 3D FORMULATION IN TERMS OF INTRINSIC 1D VARIABLES

Here we present an overview of the 3D formulation. Since we are first considering the beam as a generic elastic body, the displacement of every point in the beam can be expressed in terms of three components, each a function of three curvilinear coordinates x_1 , x_2 , and x_3 , where x_1 is a running length coordinate along the reference line of the beam. This line can be any conveniently chosen line. In elementary theory, it is normally chosen to be the locus of shear centers. However, for our purposes this choice is not viable, because the shear center does not in general exist for composite beams. Other convenient choices include the locus of aerodynamic centers, the locus of cross-sectional mass centroids, etc. For beams with a straight axis about which the initial twist takes place, choice of this axis as the reference line allows one to characterize the beam as simply initially twisted.

To make the process of dimensional reduction more understandable, we introduce 1D variables typically associated with a refined beam theory. These are associated with the average position vector of all material points in a cross-section and a frame associated with a planar cross-section of the undeformed beam at a specific value of x_1 .

It is convenient to introduce a reference frame A, in which are fixed dextral, mutually perpendicular, unit vectors \mathbf{A}_i for $i = 1, 2, 3$. The frame A is an absolute frame as far as deformation is concerned, in that the orientation of the local undeformed beam cross-section in A is a function only of x_1 and not of time t . The motion of A in an inertial frame I is, however, supposed to be known for all time. This assumption is easily relaxed for applications to multi-flexible-body dynamics; it is made only for the sake of simplifying our discussion here.

Consider the beam idealized as a reference line and a typical reference cross-section, as shown in Fig. 2. Let x_1 denote arc-length along a curved reference line \mathbf{r} for an undeformed, but initially curved and twisted beam. Let x_α denote lengths along straight lines that are orthogonal to each other and to the reference line \mathbf{r} within a cross-section $\Sigma(x_1)$. (Here and hereafter throughout this paper, unless otherwise specified, Greek indices assume values 2 and 3, while Latin indices assume values 1, 2, and 3. Repeated indices are summed over their range unless indicated otherwise.) Here a point on the undeformed beam reference line \mathbf{r} is located relative to a point fixed in frame A by the position vector $\mathbf{r}(x_1)$. At each point along \mathbf{r} define a frame \mathbf{b} in which are fixed orthogonal unit vectors \mathbf{b}_i for $i = 1, 2, 3$ such that $\mathbf{b}_2(x_1)$ and $\mathbf{b}_3(x_1)$ are tangent to the coordinate curves x_2 and x_3 at \mathbf{r} and \mathbf{b}_1 is tangent to \mathbf{r} . Each value of x_1 then specifies not only a point on \mathbf{r} but also a reference cross-section at that point, shown in green at the top the figure. The frame \mathbf{b} has an orientation that is fixed in A for any fixed value of x_1 but varies along the beam if the beam is initially curved or twisted. Notice that $x_2\mathbf{b}_2 + x_3\mathbf{b}_3 = x_\alpha\mathbf{b}_\alpha$ is the position vector of an arbitrary point within a particular cross-section relative to the point in that cross-section where \mathbf{r} intersects it. A particle of the beam is then located from a fixed point in space by the position vector

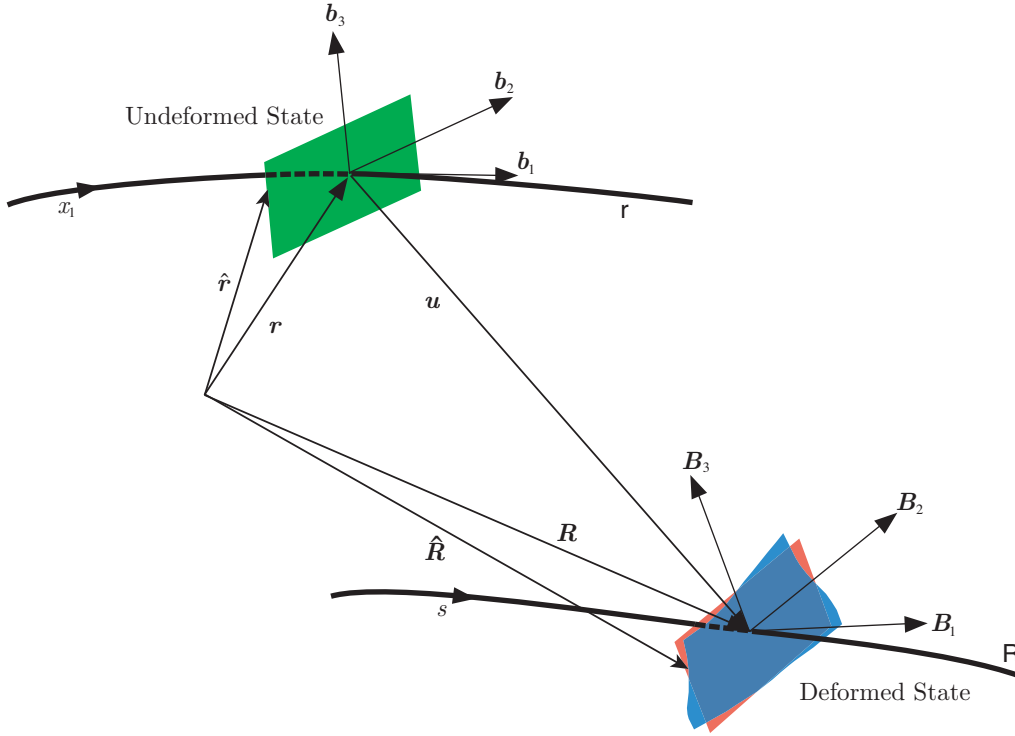


Fig. 2: Schematic of beam deformation

$\hat{\mathbf{r}}(x_1, x_2, x_3)$, given by

$$\hat{\mathbf{r}} = \mathbf{r} + x_\alpha \mathbf{b}_\alpha \quad (1)$$

Similarly, consider the configuration of the deformed beam as shown in Fig. 2. The locus of material points along \mathbf{r} has now assumed a different curved line denoted by \mathbf{R} . Let s denote arc-length along \mathbf{R} . The locus of points belonging to the initially planar reference cross-section of the undeformed beam has undergone a rigid-body translation and rotation, as well as a warping displacement. The rigid-body translation is along the vector $\mathbf{u}(x_1^*)$, the position vector from the point on the undeformed beam reference line at $x_1 = x_1^*$ to the point on the deformed beam reference line at $s = s(x_1^*)$. At each point along \mathbf{R} introduce the frame \mathbf{B} in which are fixed orthogonal unit vectors $\mathbf{B}_i(x_1)$ for $i = 1, 2, 3$, with $\mathbf{B}_1(x_1^*)$ normal to the deformed beam reference cross-sectional plane and $\mathbf{B}_\alpha(x_1^*)$ lying in this plane, shown in red at the bottom of the figure. Note that $\mathbf{B}_1 = \mathbf{B}_2 \times \mathbf{B}_3$ is not necessarily tangent to \mathbf{R} unless one adopts the Euler-Bernoulli hypothesis, here generalized to mean that the reference cross-section remains normal to \mathbf{R} when the beam is deformed. In addition to the rigid-body motion of the set of particles making up the reference cross-section of the undeformed beam, this initially plane set of particles warps, shown in blue in the figure. The frame \mathbf{B} is chosen so that the portion of the displacement relegated to the warping is small, so that the deformed beam reference cross-sectional plane is the plane that is closest to those material points of the deformed beam that make up the reference cross-section of the undeformed beam at x_1^* of the undeformed beam. We will be more precise in defining frame \mathbf{B} later, but this level of detail is sufficient presently.

In order to represent the deformed state mathematically, we must first deal with the rotation. Rotation from \mathbf{b}_i to \mathbf{B}_i is characterized in terms of the matrix of direction cosines, viz., C_{ij} , so that

$$C_{ij} = \mathbf{B}_i \cdot \mathbf{b}_j \quad (2)$$

Now the displacement field can be specified. Introduce $\mathbf{R} = \mathbf{r} + \mathbf{u}$, where $\mathbf{u} = u_i \mathbf{b}_i$ is the 1D displacement variable, i.e. the position from a point on the undeformed beam reference line to a point with the same value of x_1 on the deformed beam reference line. Now, one can represent the position of a particle in the deformed beam that had position $\hat{\mathbf{r}}$ in the undeformed beam as $\hat{\mathbf{R}}(x_1, x_2, x_3)$, given by

$$\hat{\mathbf{R}} = \mathbf{r} + \mathbf{u} + x_2 \mathbf{B}_2 + x_3 \mathbf{B}_3 + w_i \mathbf{B}_i \quad (3)$$

where $w_i = w_i(x_1, x_2, x_3)$ represents the (small) warping displacement field. Except for w_i , all unknowns in this equation depend only on x_1 . Notice that if warping is suppressed, the locus of points that were in a reference cross-sectional plane in the undeformed beam is now in the plane determined by \mathbf{B}_2 and \mathbf{B}_3 . When warping is not suppressed, it should be emphasized that the unit vectors \mathbf{B}_i , for $i = 1, 2, 3$, are orthogonal by definition and that the material lines in the deformed beam that were along \mathbf{b}_i in the undeformed beam are neither necessarily straight nor orthogonal in the deformed beam.

Thus, the 3D displacement field is expressed in terms of the displacement of the reference line \mathbf{u} , the direction cosine matrix of the cross-sectional frame C , and the warping w and its partial derivatives. (Note that here and throughout this paper, symbols without subscripts such as w are used to denote matrices having elements denoted by the corresponding symbols with subscripts, i.e. w_1 , w_2 , and w_3 .) Using the small local rotation approximation of Hodges (2006), which is adequate for blades with closed cross-sections, the six components of the 3D strain are expressible as linear functions of the 1D generalized force γ and moment strains κ . The force strains are defined such that

$$\mathbf{R}' = (1 + \gamma_{11}) \mathbf{B}_1 + 2\gamma_{1\alpha} \mathbf{B}_\alpha \quad (4)$$

where (\prime) denotes the derivative with respect to x_1 . The moment strains κ are defined as

$$\kappa = K - k \quad (5)$$

where k is the column matrix of initial twist/curvature measures in the \mathbf{b} basis, and K is the column matrix of deformed beam twist/curvature measures in the \mathbf{B} basis. Components of K which form an antisymmetric matrix $\tilde{K}_{ij} = -e_{ijl} K_l$ using the permutation symbol e_{ijk} which can be expressed in the form

$$\tilde{K} = -C' C + C \tilde{k} C \quad (6)$$

From Eqs. (4), we can find explicit expressions for the 1D generalized force strains, viz.,

$$\gamma = C(e_1 + u' + \tilde{k}u) - e_1 \quad (7)$$

where $e_1 = [1 \ 0 \ 0]^T$. Therefore, the strain energy of the cross-section or the strain energy per unit length of the beam may be written as

$$\mathcal{U} = \frac{1}{2} \langle\langle F^T \mathcal{D} F \rangle\rangle \quad (8)$$

where the angle brackets signify integration of the argument times $1 - x_2 k_3 + x_3 k_2$ over the cross-sectional plane Σ . The 3D strain components are here represented by the matrix

$$\Gamma = [\Gamma_{11} \ 2\Gamma_{12} \ 2\Gamma_{13} \ \Gamma_{22} \ 2\Gamma_{23} \ \Gamma_{33}]^T \quad (9)$$

where Γ is a function of the generalized strains, γ and κ , along with the warping w and its partial derivatives with respect to x_i . Thus, one may write that

$$\mathcal{U} = \mathcal{U}(\gamma, \kappa, w) \quad (10)$$

which is the most general form. The appearance of the column matrix w should be interpreted as w and a subset of its partial derivatives.

An expression for the velocity of every point in a typical cross-section is also needed in order to calculate the kinetic energy per unit length. Asymptotic methods have proven that the warping is of the order of the strain relative to the cross-sectional dimension. Therefore, we may neglect the influence of warping when calculating the velocity field. This in effect regards the cross-sectional plane as rigid *only for the purposes of calculating the velocity*. Elementary laws of kinematics allow us to write the velocity of a typical material point \mathbf{M} in the inertial frame \mathbf{I} in terms of motion variables or generalized velocity variables for the system of particles that make up the reference cross-section. These are the *generalized speeds* of Kane and Levinson (1985). We first introduce the column matrices that contain the measure numbers of $\boldsymbol{\omega}^{\mathbf{bI}}$ in the \mathbf{b} basis, and $\boldsymbol{\omega}^{\mathbf{BI}}$ in the \mathbf{B} basis, denoted by $\boldsymbol{\omega}$ and $\boldsymbol{\Omega}$, respectively, and related by

$$\tilde{\boldsymbol{\Omega}} = -\dot{C}C + C\tilde{\boldsymbol{\omega}}C \quad (11)$$

where $(\dot{})$ is the partial derivative with respect to time. The similarity of this equation with Eq. (6) is duly noted. Any representation for finite rotation can be used.

The reference line intersects the cross-section at point \mathbf{B}^* , so that now one can introduce the column matrix that contains the measure numbers of $\boldsymbol{v}^{\mathbf{B}^*\mathbf{I}}$, the velocity of \mathbf{B}^* in the \mathbf{B} basis, denoted by V and given by

$$V = C(v + \dot{u} + \tilde{\boldsymbol{\omega}}u) \quad (12)$$

where v is the velocity of \mathbf{b} in the inertial frame, expressed in the \mathbf{b} basis. The similarity between this relation and the strain in Eq. (7) is also apparent. With these motion variables, the inertial velocity of \mathbf{M} expressed in the \mathbf{B} basis is

$$v_{\mathbf{B}}^{\mathbf{MI}} = V + \tilde{\boldsymbol{\Omega}}\xi \quad (13)$$

where

$$\xi = p_{\mathbf{B}}^{\mathbf{M}/\mathbf{B}^*} = \begin{Bmatrix} 0 \\ x_2 \\ x_3 \end{Bmatrix} \quad (14)$$

and the kinetic energy becomes

$$\mathcal{K} = \frac{1}{2} \left(\mu V^T V - 2\mu \Omega^T \tilde{V} \bar{\xi} + \Omega^T i \Omega \right) \quad (15)$$

where μ is mass per unit length. It should be noted that the matrix i also can be written in the form

$$i = \begin{bmatrix} i_2 + i_3 & 0 & 0 \\ 0 & i_2 & i_{23} \\ 0 & i_{23} & i_3 \end{bmatrix} \quad (16)$$

where the (1,1) element is the torsional inertia, and the terms in the lower-right 2×2 sub-matrix contribute to the cross-sectional rotary inertia terms associated with bending.

Application of Hamilton's principle yields two problems, one involving variations of 1D variables γ , κ , V , and Ω , and the other involving variations of w and its first partial derivatives. The latter is a 3D problem which can be solved by taking into account the smallness of the cross-sectional length-scale a relative to the wavelength of deformation along the beam and to the characteristic length associated with initial curvature and twist, namely $R = 1/\sqrt{(k^T k)}$. The presence of the warping displacements in the strain energy makes the problem 3D. Because the warping only appears in the strain energy, the solution for the warping can be found from the static analysis (i.e. with only the strain energy). The warping is eliminated through the process of dimensional reduction. This process also precisely determines the orientation of B , so that the warping is indeed small, of the order of the strain compared to the cross-sectional dimensions. Note that the displacement field in Eq. (3), through the introduction of \mathbf{u} and the change of orientation between \mathbf{b} and B , is six times redundant. Therefore, the warping must be constrained six times. Detailed discussions of the constraints and dimensional reduction process are found in Hodges (2006). Suffice it to say here that with the choice of constraints used therein and embodied in VABS, the warping displacement is of the order of a times the strain, where a is the characteristic dimension of the cross-section. An overview of the dimensional reduction process and its output are presented next.

3. CROSS-SECTIONAL ANALYSIS

Dimensional reduction is a mathematical process that involves removing variables that depend on a number of dimensions and replacing them with other variables that depend on a smaller number of dimensions, along with explicit dependence on one or more independent variables. In a beam analysis we want to eliminate any variables that depend on cross-sectional coordinates x_2 and x_3 and in their place introduce a functional that depends explicitly on x_2 and x_3 . Thus, we need to eliminate w from the strain energy in terms of 1D variables and x_2 and x_3 . This process is well-suited for the variational-asymptotic method of Berdichevsky (1980). A cross-sectional analysis leading to a generalized Timoshenko model for initially curved and twisted anisotropic beams was first carried out by Yu *et al.* (2002a), is embodied in the computer program VABS, and is described in context of complete beam analysis in Chapter 4 of Hodges (2006).

For nonhomogeneous, anisotropic beams, VABS gives the elastic constants for a strain energy per unit length of the form

$$\mathcal{U} = \frac{1}{2} \begin{Bmatrix} \gamma_{11} \\ 2\gamma_{12} \\ 2\gamma_{13} \\ \kappa_1 \\ \kappa_2 \\ \kappa_3 \end{Bmatrix}^T \begin{bmatrix} S_{11} & S_{12} & S_{13} & S_{14} & S_{15} & S_{16} \\ S_{12} & S_{22} & S_{23} & S_{24} & S_{25} & S_{26} \\ S_{13} & S_{23} & S_{33} & S_{34} & S_{35} & S_{36} \\ S_{14} & S_{24} & S_{34} & S_{44} & S_{45} & S_{46} \\ S_{15} & S_{25} & S_{35} & S_{45} & S_{55} & S_{56} \\ S_{16} & S_{26} & S_{36} & S_{46} & S_{56} & S_{66} \end{bmatrix} \begin{Bmatrix} \gamma_{11} \\ 2\gamma_{12} \\ 2\gamma_{13} \\ \kappa_1 \\ \kappa_2 \\ \kappa_3 \end{Bmatrix} + \frac{1}{2} A_{22} \gamma_{11} \kappa_1^2 \quad (17)$$

where $A_{22} \approx S_{44} + S_{55}$. The last term represents the energy associated with the trapeze effect, accounting for the influence of the axial force caused by rotation of the rotor on the effective torsional stiffness. For slowly turning rotors, such as those of wind turbines, one may neglect this term. VABS also provides the relations for recovery of all strain and stress components over each cross-sectional model, given the solution for appropriate 1D variables at that cross-section.

A strain energy density for classical theory, i.e. without the transverse shearing variables $2\gamma_{1\alpha}$, can be found by minimization of this expression for the energy with respect to $2\gamma_{1\alpha}$ while simultaneously constraining γ_{11} and κ_i so that $2\gamma_{1\alpha} = 0$. The resulting matrix of elastic constants is only 4×4 instead of 6×6 . Although the classical theory can also be used for composite beams, it cannot achieve the accuracy of the generalized Timoshenko theory. Moreover, as shown below, classical theory must be applied at a specific reference line in order to obtain reasonably accurate results, whereas the generalized Timoshenko theory allows arbitrary choice of reference line.

4. 1D EQUATIONS FOR ROTATING WIND TURBINE BLADES

Equations resulting from the strain energy density of Eq. (17) and the kinetic energy density of Eq. (15) lead to a set of partial differential equations, derived in Chapter 5 of Hodges (2006). In this section we present these governing equations, including partial differential equations of motion and kinematics.

The partial differential equations of motion are derived in Chapter 5 of Hodges (2006) and are given as

$$\begin{aligned} F' + \tilde{K}F + f &= \dot{P} + \tilde{\Omega}P \\ M' + \tilde{K}M + (\tilde{e}_1 + \tilde{\gamma})F + m &= \dot{H} + \tilde{\Omega}H + \tilde{V}P \end{aligned} \quad (18)$$

Here the new variables are column matrices of the measure numbers of vectors expressed in the B basis: the section force F , the section moment M , the section linear momentum P , the section angular momentum H , the applied distributed force per unit length f , and the applied distributed moment per unit length m .

When the trapeze terms are neglected, Eq. (17) provides the constitutive equations (alge-

braic) for this system as

$$\begin{Bmatrix} F_1 \\ F_2 \\ F_3 \\ M_1 \\ M_2 \\ M_3 \end{Bmatrix} = \begin{bmatrix} S_{11} & S_{12} & S_{13} & S_{14} & S_{15} & S_{16} \\ S_{12} & S_{22} & S_{23} & S_{24} & S_{25} & S_{26} \\ S_{13} & S_{23} & S_{33} & S_{34} & S_{35} & S_{36} \\ S_{14} & S_{24} & S_{34} & S_{44} & S_{45} & S_{46} \\ S_{15} & S_{25} & S_{35} & S_{45} & S_{55} & S_{56} \\ S_{16} & S_{26} & S_{36} & S_{46} & S_{56} & S_{66} \end{bmatrix} \begin{Bmatrix} \gamma_{11} \\ 2\gamma_{12} \\ 2\gamma_{13} \\ \kappa_1 \\ \kappa_2 \\ \kappa_3 \end{Bmatrix} \quad (19)$$

To form a complete system, the equations of motion in Eqs. (18) and constitutive relations in Eq. (19) must be augmented by the kinematical partial differential equations, Eqs. (12) and (11) for the generalized speeds plus Eqs. (7) and (6) for the generalized strains. When a particular finite rotation formulation is used, these can be rewritten accordingly. Chapter 5 of Hodges (2006) uses Rodrigues parameters. These equations can be used in mixed form, such as the weakest form found in Eq. (5.50) of Hodges (2006). Alternatively, they can be collapsed into a set of six partial differential equations of motion in three displacement and three rotation variables, as done by Bauchau and Kang (1993). Either set is suitable for finite element discretization. Examples of finite element discretization of this set of equations can be found in the documentation for multi-flexible-body codes DYMORE (see Bauchau and Kang (1993); Bauchau (1998, 2003)) and RCAS (see, for example, Anon. (2003); Saberi *et al.* (2004)). Both codes have geometrically exact composite beam elements and use the beam cross-sectional properties from VABS.

5. EXAMPLES

5.1 A Pitfall Associated with Use of Classical Theory.

VABS provides common engineering beam models such as the classical model (a generalized Euler-Bernoulli/Saint-Venant model represented by a 4×4 stiffness matrix), a generalized Timoshenko model (represented by a 6×6 stiffness matrix), and a generalized Vlasov model (represented by a 5×5 stiffness matrix and appropriate for thin-walled open-section beams). The classical model is the simplest; it is commonly accepted that it can approximate results of the generalized Timoshenko model for static and low-frequency vibration analysis of slender beams. However, for accurate prediction using the classical model, it is necessary for the analyst to choose the reference line along the locus of generalized shear centers defined below. On the other hand, if the Timoshenko model is used to carry out the analysis, the reference line can be selected arbitrarily. In what follows, we will use an example to clarify this subtlety.

Consider a prismatic composite beam of length ℓ , clamped at $x_1 = 0$ and loaded at the tip with $F(\ell) = \hat{F}$ and $M(\ell) = \hat{M}$. The cross-sectional properties of this beam can be characterized using VABS Timoshenko model in terms of a 6×6 flexibility matrix as follows:

$$\begin{Bmatrix} \gamma \\ \kappa \end{Bmatrix} = \begin{bmatrix} R & Z \\ Z^T & T \end{bmatrix} \begin{Bmatrix} F \\ M \end{Bmatrix} \quad (20)$$

Let us denote the column matrix of infinitesimal spanwise rotation measures by θ and displacement measures by u , both expressed in the b basis. According to Hodges (2006),

the linear static behavior of this beam has the closed-form solution

$$\theta = \left[x_1 Z^T + \left(x_1 \ell - \frac{x_1^2}{2} \right) T \tilde{e}_1 \right] \hat{F} + x_1 T \hat{M} \quad (21)$$

and

$$u = \left[x_1 R + \left(x_1 \ell - \frac{x_1^2}{2} \right) Z \tilde{e}_1 - \frac{x_1^2}{2} \tilde{e}_1 Z^T - \left(\frac{x_1^2 \ell}{2} - \frac{x_1^3}{6} \right) \tilde{e}_1 T \tilde{e}_1 \right] \hat{F} + \left[x_1 Z - \frac{x_1^2}{2} \tilde{e}_1 T \right] \hat{M} \quad (22)$$

This is the most compact expression for static behavior of linearly elastic beams with full elastic coupling.

The shear center is usually defined as the point on the cross-section at which transverse shearing forces can be applied without inducing twist, θ_1 . Because of possible non-zero bending-twist couplings, i.e. when $T_{1\alpha} \neq 0$, such a point does not in general exist for composite beams. On the other hand, the *generalized shear center*, defined as the point on the cross-section at which $Z_{\alpha 1} = 0$, will always exist. At this point, transverse shear forces contribute to the twist only through the bending moments they induce.

It is noted that the origin of the cross-sectional Cartesian coordinate system is chosen arbitrarily. If we offset the origin to be at a point \mathbf{A} (a_2, a_3) in the coordinate system used to obtain Eq. (20), the flexibility matrix will be transformed according to

$$\begin{bmatrix} R_A & Z_A \\ Z_A^T & T_A \end{bmatrix} = \begin{bmatrix} R - \tilde{r} Z^T + Z \tilde{r} - \tilde{r} T \tilde{r} & Z - \tilde{r} T \\ Z^T + T \tilde{r} & T \end{bmatrix} \quad (23)$$

where the subscript A denotes that the subscripted variable is evaluated at the point A and where $r = [0 \ a_2 \ a_3]^T$. The transformed flexibility matrix in Eq. (23) can be substituted into Eqs. (21) and (22) to obtain the rotations θ_A and displacements u_A , respectively, which are the global beam behavior if the locus of point A is chosen as the reference line. It can be easily verified that

$$u_A = u - \tilde{r} \theta \quad \theta_A = \theta \quad (24)$$

which means that the displacement and rotation at some arbitrary point in the beam are invariant no matter what the choice of reference line.

On the other hand, when using the classical model one loses the freedom to use a cross-sectional model for an arbitrary reference line. The 4×4 cross-sectional flexibility matrix of the classical model can be obtained from the corresponding cross-sectional flexibility matrix of the Timoshenko model, Eq. (20), by eliminating the two rows corresponding to $2\gamma_{1\alpha}$ and the two columns corresponding to F_α . Linear static analysis using this model yields the following exact solutions for rotations and displacements:

$$\theta = \left[x_1 Z^T e_1 e_1^T + \left(x_1 \ell - \frac{x_1^2}{2} \right) T \tilde{e}_1 \right] \hat{F} + x_1 T \hat{M} \quad (25)$$

$$u_1 = \left[x_1 R_{11} e_1^T + \left(x_1 \ell - \frac{x_1^2}{2} \right) e_1^T Z \tilde{e}_1 \right] \hat{F} + x_1 e_1^T Z \hat{M} \quad (26)$$

Table 1: Differences between global displacements and rotation predicted by generalized Timoshenko and classical models

Deformation	Difference
u_1	$x_1(\hat{F}_2 R_{12} + \hat{F}_3 R_{13})$
u_2	$x_1 \left\{ \hat{F}_1 R_{12} + \hat{M}_i Z_{2i} + \hat{F}_2 (R_{22} + \ell Z_{23}) + \hat{F}_3 \left[R_{23} - \ell Z_{22} + \frac{x_1}{2} (Z_{22} + Z_{33}) \right] \right\}$
u_3	$x_1 \left\{ \hat{F}_1 R_{13} + \hat{M}_i Z_{3i} + \hat{F}_3 (R_{33} - \ell Z_{32}) + \hat{F}_2 \left[R_{23} + \ell Z_{33} - \frac{x_1}{2} (Z_{22} + Z_{33}) \right] \right\}$
θ_1	$x_1(\hat{F}_2 Z_{21} + \hat{F}_3 Z_{31})$

with $\theta = [\theta_1 \quad -u'_3 \quad u'_2]^T$ and $e_1^T Z = [Z_{11} \quad Z_{12} \quad Z_{13}]$. One can obtain u_2, u_3 from a simple integration of the second and third equations of Eq. (25). For convenience of discussion, we list the differences between u_i and θ_1 from the generalized Timoshenko and classical models in Table 1. One can make the following observations. First, the twist behavior will be predicted exactly when using the classical model if and only if the generalized shear center (the point on the cross-section at which $Z_{\alpha 1} = 0$) is chosen as the reference line. Second, the axial displacement will be predicted exactly when using the classical model if and only if $R_{1\alpha} = 0$. Finally, the classical model provides acceptable accuracy if:

1. The extension-shear couplings, $2R_{12}$ and $2R_{13}$, are negligible compared to extension bending couplings ℓZ_{13} and ℓZ_{12} , respectively.
2. The relative error in the transverse deflections caused by transverse shear flexibility is small, which is true if $3(R_{22} + Z_{23}\ell) \ll T_{33}\ell^2$ and $3(R_{33} - Z_{32}\ell) \ll T_{22}\ell^2$. The relative error in the terms coupling the transverse deflections is $6R_{23} + 3(Z_{33} - Z_{22})\ell$ relative to $2T_{23}\ell^2$; this term may or may not have an important influence.
3. The relative error in transverse deflections caused by moments (or in rotations caused by transverse shear forces) is small if $2Z_{2\alpha} \ll T_{\alpha 3}\ell$ and $2Z_{3\alpha} \ll T_{\alpha 2}\ell$.

These relations are sufficient but not all are necessary; most hold for static behavior of beams that are sufficiently slender and, by inference, for beams vibrating with sufficiently long wavelength. For example, even in the best case, if the generalized shear center is used as a reference line in a classical model, accuracy for bending modes higher than the first or second will definitely deteriorate, and more so the higher the mode. One should definitely use the generalized Timoshenko model rather than the classical one for structural dynamics applications.

5.2 Examples Using VABS, DYMORE and RCAS.

To demonstrate the application of VABS to model wind turbine blades, we will use VABS to obtain the properties of a typical wind turbine blade cross-section, as sketched in Fig. 3. The outline of the blade is a VR-7 airfoil (see <http://www.nasg.com/afdb/list-airfoil-e.phtml>) with chord length 20.2 inches and the web located 8.4025 in. from the leading edge. Properties of the materials used to make the different components of this blade are

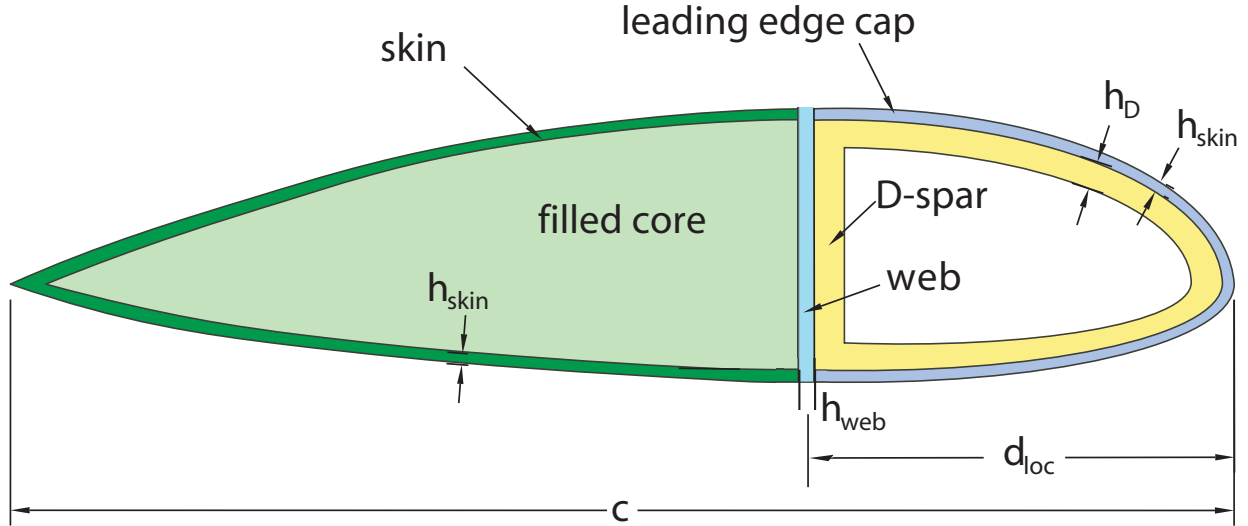


Fig. 3: Sketch of a cross-section for a typical wind turbine blade

Table 2: The materials composing the wind turbine blade

Components	Material	Thickness (in)
Leading edge cap	Titanium	0.04
D-Spar	Graphite/Epoxy	0.35
Web	Graphite/Epoxy	0.04
Trailing edge skin	Graphite/Epoxy	0.04
Fill core	Nomex Honeycomb	N/A

listed in Table 2, where Titanium is assumed to be isotropic and both Graphite/Epoxy and Nomex honeycomb are taken to be transversely isotropic. Their material properties including density and elastic constants are given in Table 3. The layup orientations for the D-Spar are $[45^\circ / -45^\circ / 0^\circ / 0^\circ / 0^\circ]$ from outside to inside. The layup angle is 45° for the trailing edge skin and 0° for the web.

The cross-section is meshed for the running of VABS as depicted in Fig. 4, with 890 8-noded quadrilateral elements. The shear center does not exist for this section, but the generalized shear center is located at a point 5.889 in. back and 0.65789 in. up from the leading edge. VABS was run with the origin of the sectional coordinate system reset to this point. Although

Table 3: The material properties

Material	Density ($\times 10^{-4}$ lb.-sec ² /in ⁴)	Elastic properties
Titanium	4.220147	$E = 14.94977$ Mpsi, $\nu = 0.34$
Graphite/Epoxy	1.49717	$E_l = 26.25182$ Mpsi, $\nu_{lt} = 0.28$ $E_t = 1.493888$ Mpsi, $\nu_{tt} = 0.33$ $G_{lt} = 1.039920$ MPsi
Nomex Honeycomb	0.059912	$G_{lt} = 47$ Kpsi, $\nu_{lt} = \nu_{tt} = 0.30$ $E_l = E_t = 28$ Kpsi

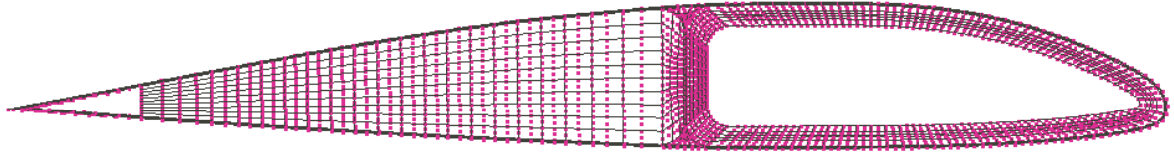


Fig. 4: Wind turbine blade cross-sectional mesh (to scale)

the choice of reference line does not affect global results of the beam calculations, such as natural frequencies, when obtained from the generalized Timoshenko model (a 6×6 matrix of cross-sectional stiffnesses), this choice does affect the accuracy of results obtained from the classical theory (a 4×4 matrix of cross-sectional stiffnesses).

The sectional mass properties calculated using VABS are

$$\begin{aligned}
\mu &= 1.54601 \times 10^{-3} \text{ lb.-sec}^2/\text{in.}^2 \\
i_2 &= 1.28544 \times 10^{-3} \text{ lb.-sec}^2 \\
i_3 &= 2.68960 \times 10^{-2} \text{ lb.-sec}^2 \\
i_{23} &= 1.01532 \times 10^{-4} \text{ lb.-sec}^2
\end{aligned} \tag{27}$$

where μ is the mass per unit length, i_2 is the mass moment of inertia about the direction along the chordline, and i_3 is the mass moment of inertia about the perpendicular direction. The center of mass is slightly off the generalized shear center and is located at $x_2 = -0.00351124$ in. and $x_3 = -0.196410$ in.

The generalized Timoshenko model obtained from VABS for this blade section is represented by the following matrix of cross-sectional stiffness constants:

$$S = \begin{bmatrix} 128.550 & -0.651479 & 0.026700 & -1.17823 & 25.0459 & -168.948 \\ -0.651479 & 9.68119 & -0.414611 & 0.021110 & 0.706635 & 1.03049 \\ 0.026700 & -0.414611 & 1.44328 & -0.001493 & -0.054592 & 0.116498 \\ -1.17823 & 0.021110 & -0.001493 & 34.5784 & 1.30984 & 1.36493 \\ 25.0459 & 0.706635 & -0.054592 & 1.30984 & 91.8417 & 25.3056 \\ -168.948 & 1.03049 & 0.116498 & 1.36493 & 25.3056 & 1492.29 \end{bmatrix} \times 10^6 \tag{28}$$

where the units associated with stiffness values are S_{ij} (lb.), $S_{i,j+3}$ (lb.-in.), and $S_{i+3,j+3}$ (lb.-in.²) for $i, j = 1, 2, 3$. It should be noted that the cross-sectional matrix from classical theory is obtained by striking the second and third rows and columns from the inverse of the 6×6 cross-sectional matrix in Eq. (28) and inverting the resulting 4×4 matrix.

Having these sectional properties, we are ready to perform all types of analysis related with the wind turbine blade. Moreover, we can define a beam element using this information in a multi-flexible-body code so that the dynamic behavior of a wind turbine with such blades can be simulated. For example, considering a blade having such a section with a span of 404 in., one can easily calculate the vibration modes and corresponding frequencies of this blade when it rotates with different angular speeds. Fig. 5 shows the fan plot

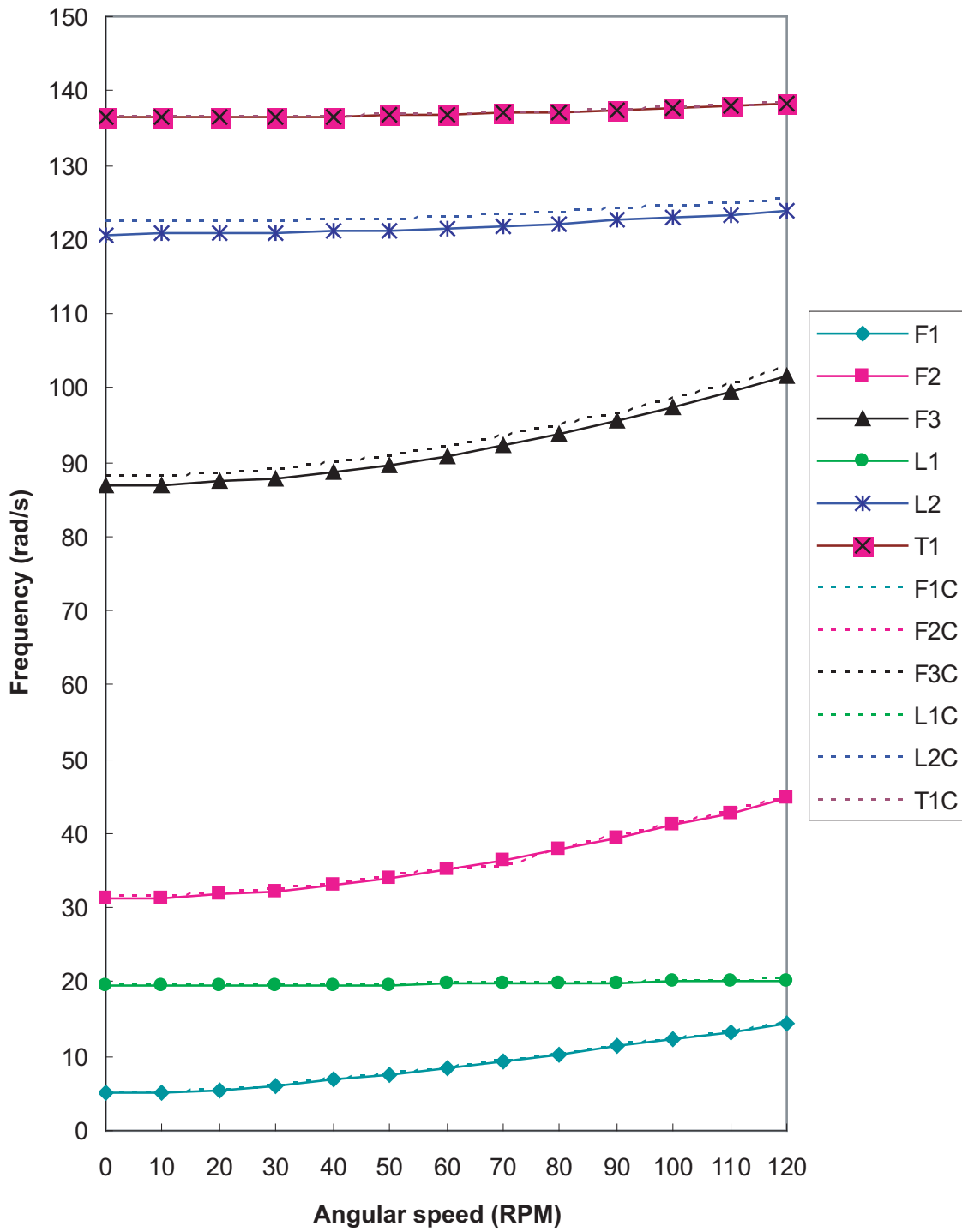


Fig. 5: Fan plot of a wind turbine blade

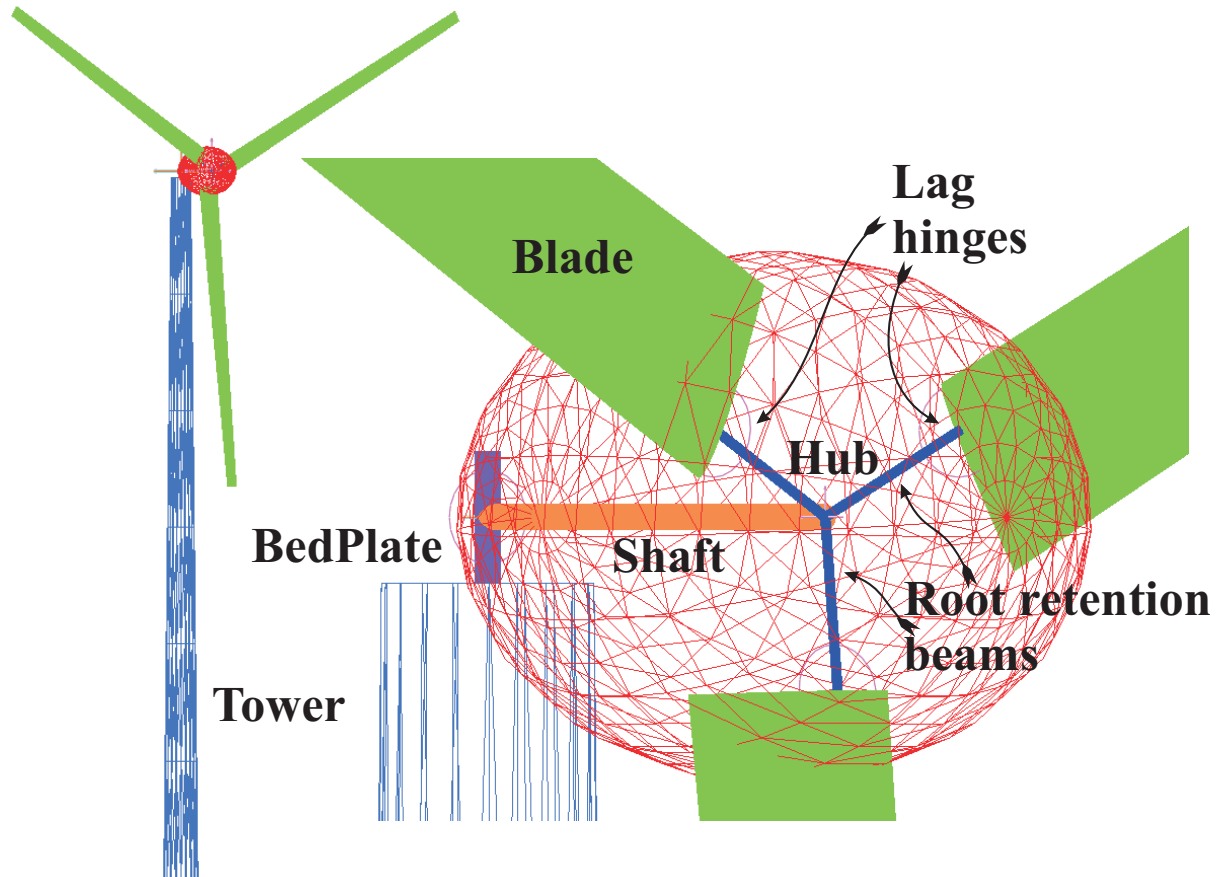


Fig. 6: Schematic of a wind turbine

of the first six modes, using both classical and generalized Timoshenko theories (F1: first flapping mode; F2: second flapping mode; F3: third flapping mode; L1: first lagging mode; L2: second lagging mode; T1: first feathering or torsional mode) of the blade clamped to a shaft rotating with different angular speeds. These results have been obtained from DYMORE, but essentially identical results are obtained from RCAS. It can be observed from the plot that the flapping frequencies change with the angular speed pretty significantly, yet the lagging and feathering/torsional frequencies do not vary nearly as much with angular speed. It is also evident that as one looks at the frequencies of modes dominated by bending, results from classical theory are slightly stiffer, and the higher the frequency (or the shorter the wavelength) the less accurate they are. If the beam becomes fatter, the difference will be more significant.

For the purpose of demonstrating that a complete wind turbine can be simulated within the present methodology, we use DYMORE to hook three identical blades onto a tower used by Bauchau and Wang (2006) to build the wind turbine model depicted in Fig. 6. The rotor is initially rotating at 90 RPM, and the angular speed is suddenly decreased to 80 RPM. We can simulate the dynamic behavior during and after this event to evaluate whether the system can withstand such a change. Please note that for simplicity, we do not consider aerodynamic loads in this simulation. All the time histories of displacement, force, and mo-

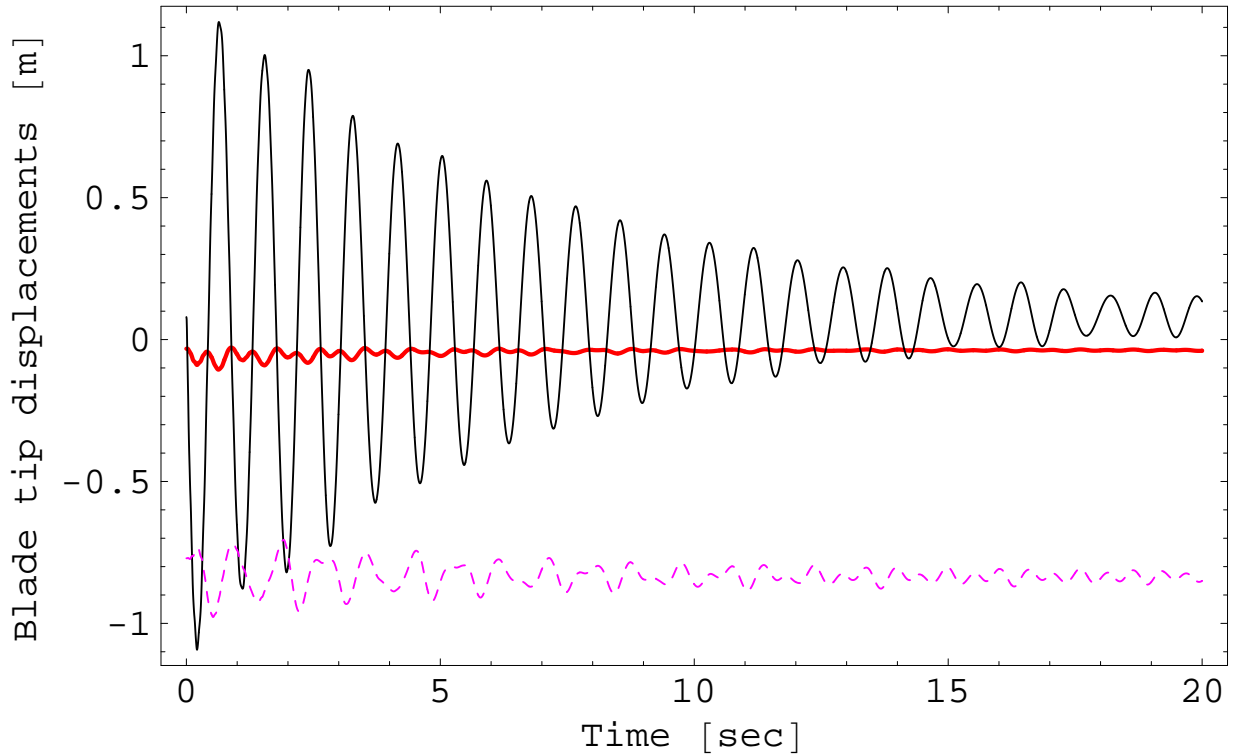


Fig. 7: Time history of blade tip displacements. Red thick line: axial; black solid line: lateral; dashed purple line: transverse

ment can be predicted. In Figs. 7, 8 and 9, we plot the time histories of elastic displacement components at the tip of the blade and the section force and moment components at the blade root, respectively. Such information provides important information for wind turbine design and analysis.

6. CONCLUDING REMARKS

A general methodology for analyzing composite beams such as wind-turbine and helicopter blades has been presented. The methodology accounts for generally anisotropic materials and arbitrary cross-sectional geometry. A rigorous asymptotic dimensional reduction procedure splits the underlying 3D problem into a 1D beam problem and a 2D cross-sectional problem, leading to significant reduction in computational effort vis-à-vis 3D finite elements. The cross-sectional analysis is implemented in VABS. The cross-sectional model output by VABS is nonlinear, but because the angular speed is generally small for wind-turbine rotors, one may discard results from the nonlinear part of the cross-sectional model, which are dominated by the trapeze effect. The resulting model then is a set of cross-sectional elastic constants for each modeled section that can be used in multi-flexible-body codes, such as DYMORE and RCAS, both of which use geometrically-exact 1D finite elements. The 1D results obtained can be used for stress recovery for each modeled cross-section. Results obtained demonstrate that the methodology can model realistic blades. When coupled with appropriate models for the aerodynamics and power generation equipment, the approach is

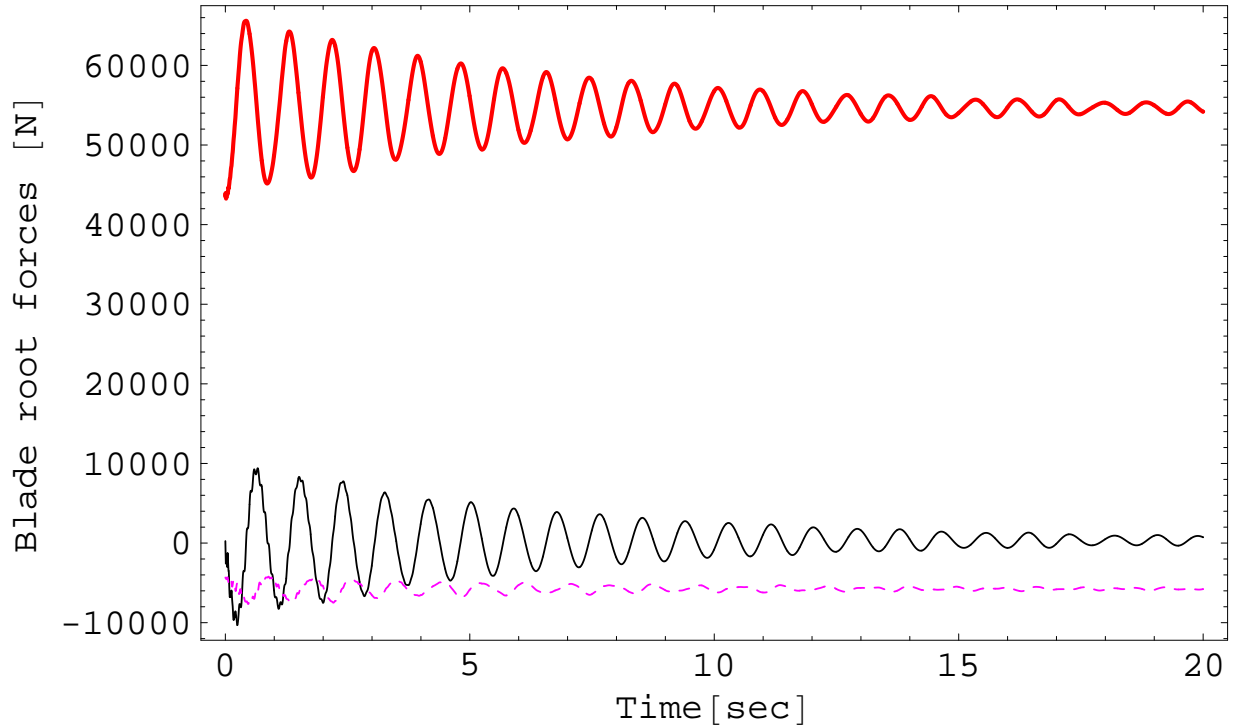


Fig. 8: Time history of blade root forces. Red thick line: axial; black solid line: lateral; dashed purple line: transverse

sufficiently powerful to calculate the dynamic behavior of complete wind turbines.

ACKNOWLEDGEMENT

The authors gratefully acknowledge nearly two decades of support from the U.S. Army and the National Rotorcraft Technology Center at the Ames Research Center.

References

- Anon. (2003). RCAS theory manual, version 2.0. Technical Report USAAMCOM/AFDD TR 02-A-005, U.S. Army Aviation and Missile Command, Moffett Field, California.
- Bauchau, O. (1998). Computational schemes for flexible, nonlinear multi-body systems. *Multibody System Dynamics* 2, 169–225.
- Bauchau, O. A. (2003). DYMORE user's and theory manual. Technical Report <http://www.ae.gatech.edu/~obauchau/dymore/dymore.html>.
- Bauchau, O. A. and Kang, N. K. (1993). A multibody formulation for helicopter structural dynamic analysis. *Journal of the American Helicopter Society* 38, 3–14.

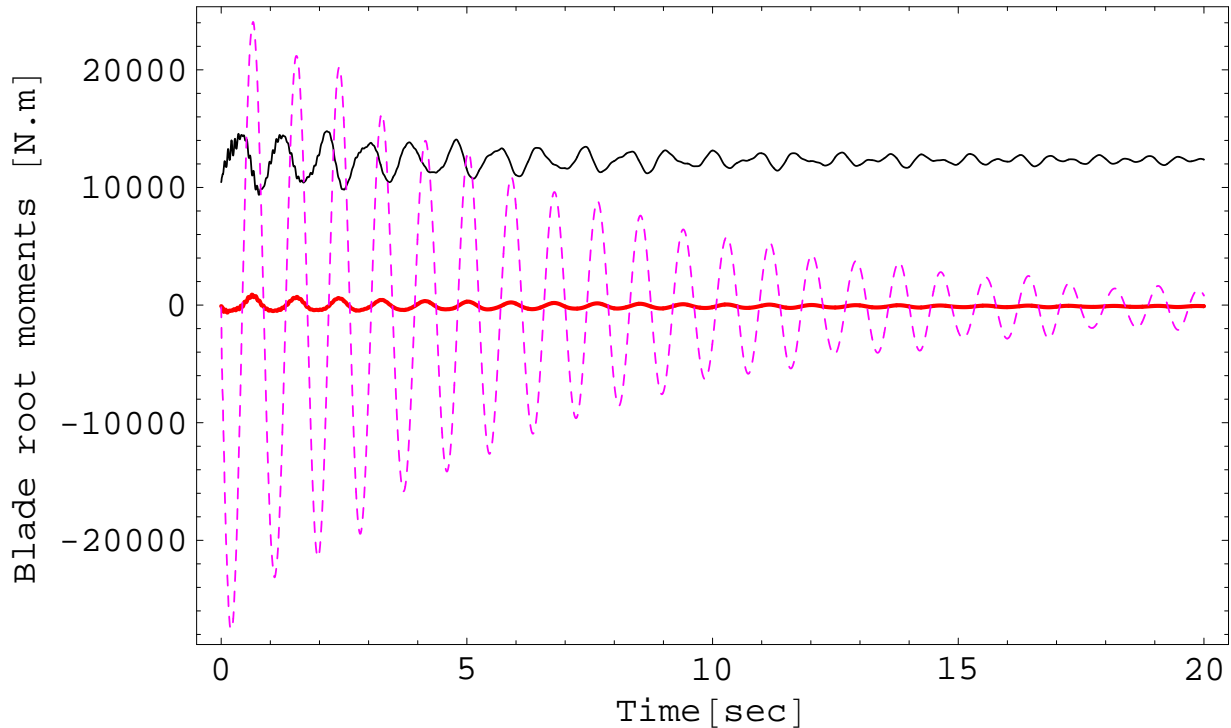


Fig. 9: Time history of blade root moments. Red thick line: axial; black solid line: lateral; dashed purple line: transverse

Bauchau, O. A. and Wang, J. (2006). Stability analysis of complex multibody systems. *Journal of Computational and Nonlinear Dynamics* 1, 71–80.

Berdichevsky, V. L. (1980). Variational-asymptotic method of constructing the nonlinear shell theory. In *Theory of Shells*, 137–161. North-Holland Publishing Company.

Borri, M. and Mantegazza, P. (1985). Some contributions on structural and dynamic modeling of helicopter rotor blades. *l'Aerotecnica Missili e Spazio* 64, 143 – 154.

Cesnik, C. E. S. and Hodges, D. H. (1993). Stiffness constants for initially twisted and curved composite beams. *Applied Mechanics Reviews* 46, S211 – S220.

Cesnik, C. E. S. and Hodges, D. H. (1994). Variational-asymptotical analysis of initially twisted and curved composite beams. *International Journal for Engineering Analysis and Design* 1, 177 – 187.

Cesnik, C. E. S. and Hodges, D. H. (1995). Stiffness constants for composite beams including large initial twist and curvature effects. *Applied Mechanics Reviews* 48, S61 – S67.

Cesnik, C. E. S. and Hodges, D. H. (1997). VABS: a new concept for composite rotor blade cross-sectional modeling. *Journal of the American Helicopter Society* 42, 27 – 38.

Cesnik, C. E. S. and Shin, S.-J. (2001). On the modeling of active helicopter blades. *International Journal of Solids and Structures* 38, 1765 – 1789.

- Danielson, D. A. and Hodges, D. H. (1987). Nonlinear beam kinematics by decomposition of the rotation tensor. *Journal of Applied Mechanics* 54, 258 – 262.
- Giavotto, V., Borri, M., Mantegazza, P., Ghiringhelli, G., Carmaschi, V., Maffioli, G. C. and Mussi, F. (1983). Anisotropic beam theory and applications. *Computers and Structures* 16, 403 – 413.
- Hodges, D. H. (2006). *Nonlinear Composite Beam Theory*. AIAA, Reston, Virginia.
- Hodges, D. H., Atilgan, A. R., Cesnik, C. E. S. and Fulton, M. V. (1992). On a simplified strain energy function for geometrically nonlinear behaviour of anisotropic beams. *Composites Engineering* 2, 513 – 526.
- Kane, T. R. and Levinson, D. A. (1985). *Dynamics: Theory and Applications*. McGraw-Hill Book Company, New York, New York.
- Kosmatka, J. B. and Friedmann, P. P. (1989). Vibration analysis of composite turbopropellers using a nonlinear beam-type finite-element approach. *AIAA Journal* 27, 1606–1614.
- Popescu, B. and Hodges, D. H. (1999a). Asymptotic treatment of the trapeze effect in finite element cross-sectional analysis of composite beams. *International Journal of Non-Linear Mechanics* 34, 709–721.
- Popescu, B. and Hodges, D. H. (1999b). On asymptotically correct Timoshenko-like anisotropic beam theory. *International Journal of Solids and Structures* 37, 535–558.
- Popescu, B., Hodges, D. H. and Cesnik, C. E. S. (2000). Obliqueness effects in asymptotic cross-sectional analysis of composite beams. *Computers and Structures* 76, 533 – 543.
- Saberi, H. A., Khoshlahjeh, M., Ormiston, R. A. and Rutkowski, M. J. (2004). RCAS overview and application to advanced rotorcraft problems. In 4th Decennial Specialists' Conference on Aeromechanics, San Francisco, California, January 21–23. American Helicopter Society.
- Volovoi, V. V., Hodges, D. H., Cesnik, C. E. S. and Popescu, B. (2001). Assessment of beam modeling methods for rotor blade applications. *Mathematical and Computer Modelling* 33, 1099 – 1112.
- Yu, W., Hodges, D. H., Volovoi, V. V. and Cesnik, C. E. S. (2002a). On Timoshenko-like modeling of initially curved and twisted composite beams. *International Journal of Solids and Structures* 39, 5101 – 5121.
- Yu, W., Volovoi, V. V., Hodges, D. H. and Hong, X. (2002b). Validation of the variational asymptotic beam sectional (VABS) analysis. *AIAA Journal* 40, 2105 – 2112.